PCCP

Accepted Manuscript

ROYAL SOCIETY OF CHEMISTRY

www.rsc.org/pccp

Nature of Flocculation and Tactoid Formation in Montmorillonite: The Role of pH

M. Segad,*,† T. Åkesson,‡ B. Cabane,¶ and Bo Jönsson‡

Advanced Light Source, Lawrence Berkeley National Laboratory, Berkeley, California 94720, United States, Theoretical Chemistry, Chemical Center, Lund University, POB 124, S-22100 Lund, Sweden, and ESPCI, 10 Rue Vauquelin, 75231 Paris Cedex 5, France

E-mail: MSegadMeehdi@lbl.gov;M.Segad@gmail.com

Abstract

The dissolution and swelling properties of montmorillonite at different pH have been studied, using small angle X-ray scattering (SAXS), imaging and osmotic stress methods combined with Monte Carlo simulations. The acidity of montmorillonite dispersions has been varied as well as the counterions to the net negatively charged platelets. At low pH, Na montmorillonite dissolves and among other species Al^{3+} is released, hydrated, polymerized and then it replaces the counterions in the clay. This dramatically changes the microstructure of Na montmorillonite, which instead of having fully exfoliated platelets, turns into a structure of aggregated platelets, so-called tactoids. Montmorillonite dispersion still has a significant extra-lamellar swelling among the tactoids due to the presence of very small nanoplatelets.

Keywords: X-ray scattering, pH, Osmotic stress, MC simulations, Clay aggregates.

*To whom correspondence should be addressed
†Advanced Light Source
‡Lund University
¶ESPCI

Introduction

The flocculation of clay platelets has been extensively studied and a number of tentative flocculation mechanisms have been proposed.[1] Freundlich et al.,[2] Hofmann et al.[3] and Langmuir[4] all observed flocculation in clay-water systems. They observed both the formation of tactoids, *i.e.* a handful of platelets stacked parallel to each other as well as a more extended gelation, and concluded that the flocculation of clay is more complex than in most other colloidal systems. van Olphen[5] proposed that under certain circumstances, *e.g.* acidity and low ionic strengths, the edges of the platelets carry a positive charge responsible for the gel formation. Thus, he attributed the gel formation to the attraction between the negatively charged faces and the positively charged edges rather than an attraction between the faces of platelets. The formation of tactoid is a special form of structurally well defined flocculation. It is important for nanotechnology application[6] and for increasing the hydraulic permeability and the acidity in soils.[7] The latter is one of the most pressing problems in agricultural practices and clay minerals.[8,9]

Soil acidification can be accelerated through mining, acid rain and pollution from industrial sources. The impact of these factors has been observed in the Netherlands,[10] where soil acidity and salinity have been considered as critical parameters affecting the physical and chemical properties of clay and has initiated a range of early studies.[11–14] The hydraulic conductivity of the clay[15–17] and its swelling capacity[18–21] are important factors both with respect to soil problems and for nuclear waste confinement. Underground nuclear repositories will eventually be surrounded by ground or sea water and in both cases an ionic competition between mono- and divalent counterions will take place in the clay.[22] Under these conditions, the formation of tactoids plays a crucial role for the hydraulic permeability.

The effect of protons (pH $\leq$ 5) on the microstructure and swelling behavior of montmorillonite is not yet well understood. One problem is that the edge charge distribution probably has a profound effect on the flocculation or aggregation of montmorillonite platelets; still the edge charge distribution remains unknown. To accurately determine the structure over

micro-to-nanometer range, see Fig. 1, resolving the aggregation number of platelets in a tactoid is essential. To the best of our knowledge, no detailed study has been performed on tactoid size, microstructure and swelling behavior of montmorillonite at different pH values and in the presence of NaCl (10−30 mM). In this work, we try to shed some light on these properties using small angle X-ray scattering (SAXS), imaging and osmotic swelling methods combined with Monte Carlo simulations (MC).

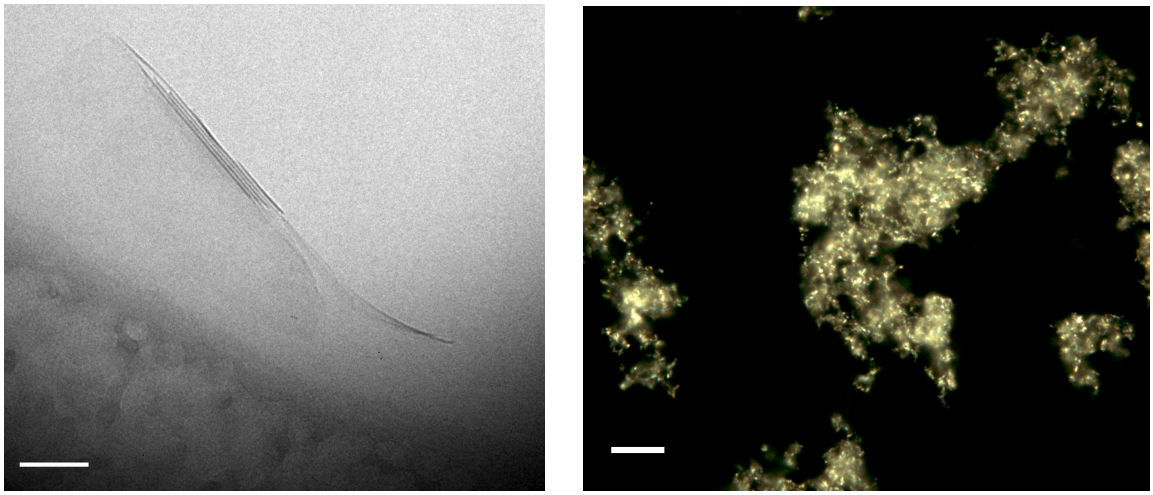

Fig. 1: Left: Cryo-TEM image of tactoid in calcium montmorillonite where small nanoplatelets form a smaller tactoid. The bar in the lower left corner corresponds to 40 nm. Right: Microscope image obtained from Na montmorillonite in pure water at pH=2 taken from dialysis experiment after one year of equilibration. Scale bar in the lower left corner corresponds to 10 μm.

Experimental Section

The source of swelling smectite used throughout this work was Wyoming bentonite (MX-80). Analytical grade sodium chloride (purity, 99.5%) was purchased from MERCK and deionized water was used to prepare the solutions. Hydrochloric acid (37% HCl) was purchased from MERCK used for adjusting pH. The double junction pH combination electrode used to measure pH was calibrated at 25 °C in buffer solutions of pH 4, 7 and 10. The reported accuracy was ±0.02. SnakeSkin dialysis tubing (3.5K MWCO, 1 mils) was bought from PIERCE.

Purification of Na montmorillonite

Na montmorillonite was obtained from Wyoming bentonite after a purification process: 20 g of MX-80 was dispersed in 2 L of deionized water and allowed to stand until the large particles, $> 2\mu$m, had sedimented after which the rest of the suspension was recovered. In order to remove most of the multivalent ions, this suspension was washed by addition of 1 M NaCl solution three times: each time the clay was mixed with the aqueous salt solution, left to settle and the supernatant was removed. Then the clay suspension was washed three times with deionized water. Each time sodium montmorillonite was left to settle for at least a week and the middle part was collected through aspiration. This step resulted in a fractionation of the clay according to sedimentation rates, and therefore according to platelets size (*i.e.* the effective diameter, $D_{eff} \sim 400$ nm).[23,24] Na montmorillonite suspensions were transferred to dialysis membranes and placed in plastic containers with deionized water. The water was changed daily until the conductivity was below 10 μS/cm. The final Na montmorillonite clay was used as dispersions or dried at 60 °C.

Sample Preparation

The SnakeSkin dialysis tubings, were cut to appropriate length (8 cm) and put into deionized water for 24 h. One end of the tubing was folded over twice and attached. Na montmorillonite (0.3−0.5 g) was added as a dry powder, and the tubing was rolled up in the open end and pressed slightly to remove the air inside the pocket and then folded over twice and attached. The tubings were placed in beakers containing 500 ml of deionized water at various pH (*i.e.* 2−6) with salt free solution or with different NaCl concentrations (10, 30 or 300 mM). These beakers were placed then in a shaking incubator hood system (from Bühler-Germany) at room temperature (25 °C) up to three months and/or a year. In the free swelling series, 0.1 and 0.3 g were dispersed into separate glass tubes with 10 ml of deionized water at pH 4 and 6 with 25 mM NaCl or with salt free system. These tubes were shaken until the clay has completely exfoliated and then left to equilibrate at 25 °C for four months.

Small Angle X-ray Scattering (SAXS)

The small angle X-ray scattering (SAXS) experiments were performed at the synchrotron radiation facility MAX IV in Lund using beamline I911-4.[25] A monochromatic beam of 0.91 Å wavelength was used together with point collimation and a two-dimensional position-sensitive detector. The SAXS data were analyzed using FIT2D. This is a viewing and analyzing program that allows calibration of the beam center, sample-to-detector distance and then integrating the 2D WAXS/SAXS images to 1D scattering data.[26] The sample to detector distance was 1.9 m ($0.1 < q < 4\ \mathrm{nm}^{-1}$). Clay samples at varying pH values and NaCl concentrations were taken from dialysis experiments. The clay dispersions were measured in 1 mm quartz capillaries. The background scattering of pure water at different pH and salt concentrations were subtracted.

The number of montmorillonite platelets per tactoid or aggregate, N, can be estimated from the scattering peaks by applying the Scherrer formula.[23,27] A model with an assumption of a Lorentzian line shape has been approximated to the scattering function based on that formula as follows:

$$q^2 I(q) \ \propto \ \frac{w}{(q - q_{max})^2 + w^2} \tag{1}$$

where $I(q)$ is the scattering intensity and w a measure of the width. The width at half maximum of the peak is equal to $2w$ and the average number of platelets per tactoid can be expressed as $\langle N \rangle \approx q_{max}/w$.[28]

Monte Carlo Simulations

The finite sized platelets are traditionally treated as infinite rigid objects in any theoretical calculations.[22,29] Another simplification is that the charged groups on or in the platelets are treated as uniformly smeared out. The actual surface net charge is approximately known from the cation exchange capacity[21,30] to be of the order of $0.1{-}0.2\ \mathrm{C/m^2}$. A further simplification,

and in fact a necessary one in order to make simulations viable, is to treat the aqueous phase as a dielectric continuum characterized by its relative dielectric permittivity $\epsilon_r = 78$. In the present study we treat any mobile charges as hard cores carrying an appropriate charge of +1, +2, +3 or -1. The montmorillonite model in Fig. 2 is assumed to be in equilibrium

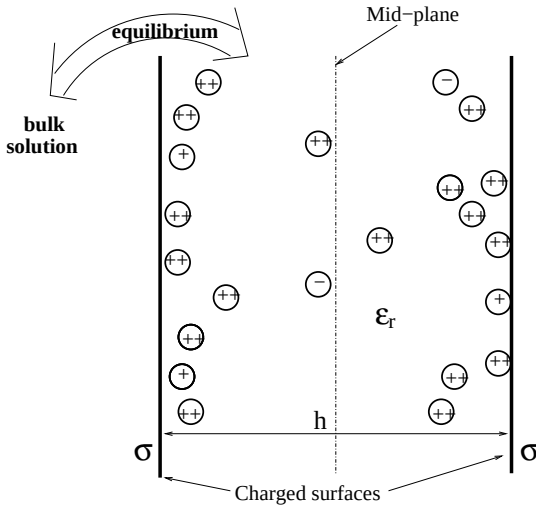

Fig. 2: Schematic picture of montmorillonite platelets with neutralizing counterions as well as salt ions described as charged hard spheres with a diameter of 0.4 nm and water is modeled as a dielectric continuum. The two infinite parallel walls have a uniform surface charge density, σ.

with an infinite salt reservoir of known salt concentration (bulk solution). The interaction, between two particles i and j separated by a distance r, can be formally written as,

$$u(r) = \begin{cases} \dfrac{Z_i Z_j e^2}{4\pi\varepsilon_o\varepsilon_r r} & r > d_{hc} \\ \infty & r \leq d_{hc} \end{cases} \tag{2}$$

where Z_i is the ion valency, e the elementary charge, ϵ_o the permittivity of vacuum and $d_{hc} = 0.4$ nm is the ion diameter chosen to be the same for all ions. The ions also interact with the charged walls and an external potential is included in order to take care of the interactions ranging outside the simulation box.[31] The osmotic pressure of the confined solution, Π^{conf}, may be calculated according to:[31,32]

$$\Pi^{conf} = k_B T \sum_i c_i(\text{mp}) + \Pi^{corr} + \Pi^{hc} \tag{3}$$

where k_B is the Boltzmann factor, T the temperature equal to 298 K, c_i is the concentration of species i and mp stands for mid-plane. The term Π^{corr} comes from the fact that ions on either side of the mid-plane correlate and give an attractive contribution to the pressure. The finite ion size, d_{hc}, gives rise to the term Π^{hc}. Equation (3) gives the osmotic pressure in the confined region and the *net* osmotic pressure is,

$$\Pi_{net} = \Pi^{conf} - \Pi^{bulk} \tag{4}$$

The bulk pressure is calculated for a bulk with the same chemical potential(s) as the double layer. Bulk simulations are performed in the canonical ensemble, where the osmotic pressure is calculated from the virial[33,34] and the chemical potential is obtained via Widom's perturbation technique.[35]

Results and Discussion

Stability of Montmorillonite

In order to study the stability of silicate platelets under acidic conditions, a fixed amount of Na montmorillonite (0.3 g) was placed in a pocket of semi-permeable membrane and the pocket was immersed into a beaker with deionized water. The beaker was shaken for approximately three months, after which the solution was analyzed by the inductively coupled plasma atomic emission spectroscopy (ICP-AES). The dialysis pocket, in each beaker, is in equilibrium with the bulk solution, as the solution has not been exchanged. Thus, the experimental results reported in Table 1 are of batch type. In Table 1, one can see that the acidity of the bulk solution (pH=4) leads to a slow dissolution of montmorillonite platelets. One can also notice that several Mg^{2+} and Al^{3+} cations are released at pH=2, which most likely indicates there is an exchange of counterions. That is, divalent and not least trivalent ions replace the Na^{+} ions as counterions in montmorillonite clay. The data in Table 1 are

in fair agreement with the results published by Tounassat et al.[36,37] and Rozalen et al.[38] considering that the samples have been prepared using different protocols.

Table 1: ICP-AES analysis of the batch solution of Na montmorillonite placed into a semi-permeable pocket at pH=2 and pH=4 after 3 months. Sample at pH=7 is taken from a polyethylene glycol (PEG)-stressed solution with 10 and 25 % PEG. Numbers show the concentration in μM.

Smectite Dispersions	Si	Al	Fe	Mg
Na montmorillonite at pH=7	4	1	2	0
Na montmorillonite at pH=4	280	0	3	2
Na montmorillonite at pH=2	950	180	40	63

Scattering Spectra of Montmorillonite Dispersions

Small angle X-ray scattering together with osmotic stress experiments usually give a good picture of the structure in a dispersion. The former probes the system on a microscopic level, while the latter provides macroscopic information. Fig. 3 clearly shows that scattering peaks appear at low pH signaling the formation of tactoids. The original clay in Fig. 3 is a pure Na montmorillonite, but once it has equilibrated at sufficiently low pH, it exchanges its monovalent counterions for multivalent ones. Thus, two distinct peaks can be seen in Fig. 3 with $\langle N \rangle \simeq 9$ at pH 2 and $\langle N \rangle \simeq 6$ at pH 3, while at pH 4 the width of SAXS shoulder indicates that the nanoplatelets are still not isolated. Surprisingly, the peak position at pH 2 and 3 corresponds to a repeat distance of approximately 2.2 nm, which is larger than that observed in Ca/Mg montmorillonite. In the latter case, the repeat distance was 1.9 nm where an approximate water layer of $\simeq$ 1 nm is predicted from MC simulations of infinite charged platelets.[22,24,28,29]

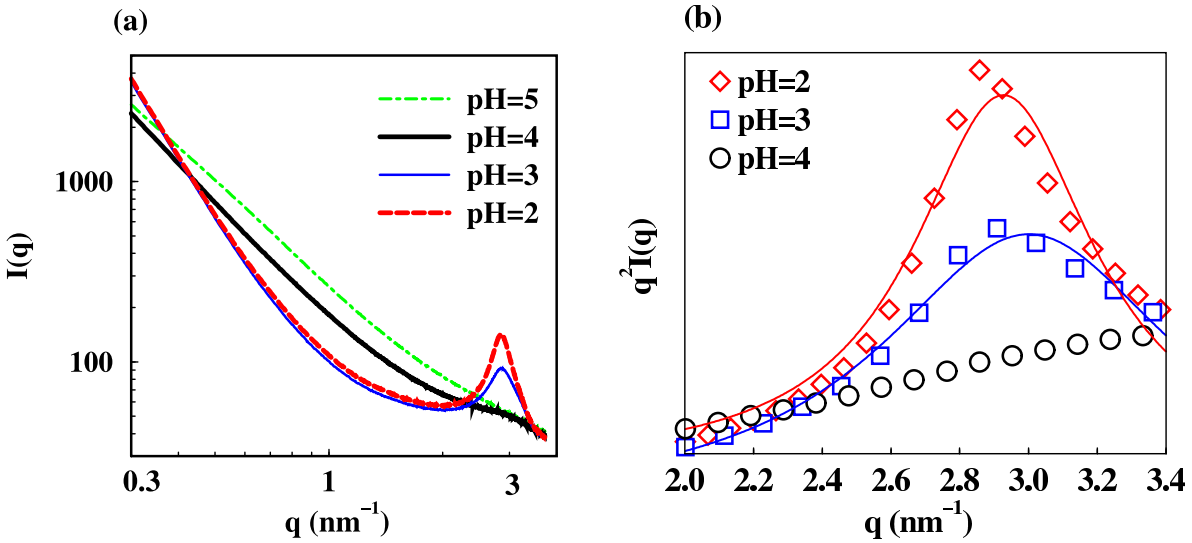

Fig. 3: (a) SAXS spectra of Na montmorillonite equilibrated in dialysis pockets with aqueous solutions at different pH as indicated in the graph. (b) Magnification of the high-q range. The fitting procedure gives $\langle N \rangle \simeq 9$ at pH=2 and $\langle N \rangle \simeq 6$ at pH=3, while at pH 4 the peak broadness prohibits an application of the fitting procedure. The solid lines are fits to equation (1).

The competition between monovalent and multivalent counterions is that even a relatively low concentration of divalent or trivalent cations in the bulk is enough for a virtually complete exchange of counterions in the dialysis pocket. To demonstrate this a small amount of NaCl has been added to the beaker in order to maintain the clay dispersion dominates by sodium counterions. With 10 mM of NaCl and pH 2 in the bulk solution there is still a peak at $q \approx 2.9$ nm^{-1}, but it is much less distinct than in a salt free system. As can be seen in Fig.

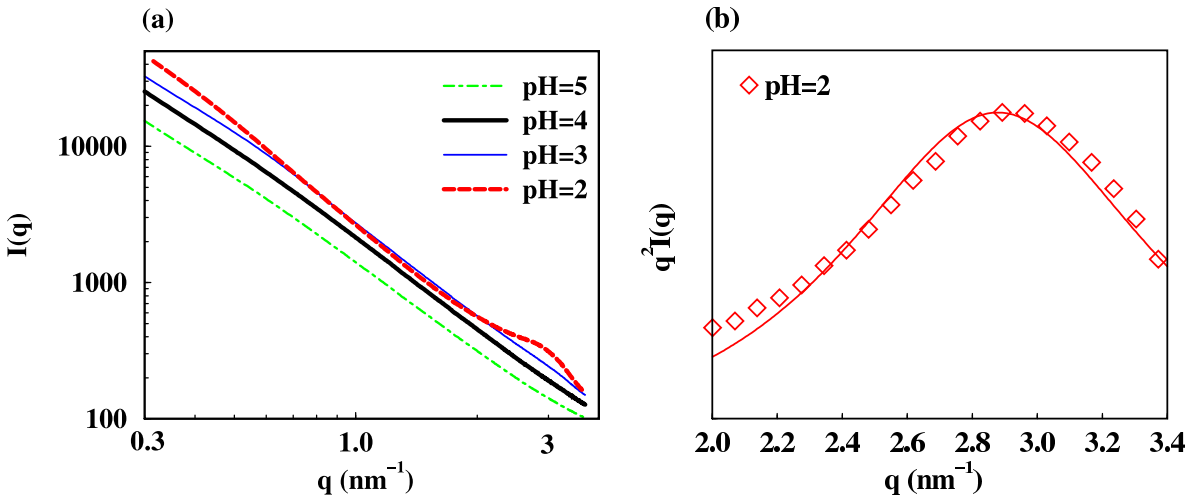

Fig. 4: (a) SAXS spectra of Na montmorillonite equilibrated in dialysis pockets with a 10 mM NaCl solution at different pH. (b) The fitting procedure gives $\langle N \rangle \simeq 5$ at pH=2. The solid lines are fits to equation (1).

4, the fitting procedure gives $\simeq 5$ platelets into a tactoid, whereas the peak at pH=3 almost vanished. Increasing the NaCl concentration in the beaker to 30 mM has no observable effect on the scattering data (spectra not shown). It should be mentioned that SAXS spectra in Fig. 4a have roughly the same power law slope $\sim q^{-2}$. This is in contrast to Fig. 3a, where the scattering curves at pH 2 and 3 show a significantly steeper slope $I(q) \propto q^{-2.8}$, indicating a change in the structure of montmorillonite clay, in agreement with SAXS data published recently *cf.* ref 40.

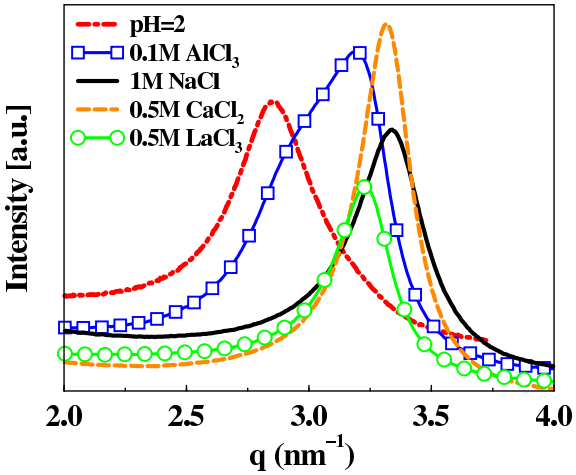

Fig. 5: X-ray scattering spectra of Na montmorillonite dispersions equilibrated in dialysis pockets with various salt solutions at neutral pH and at pH=2. See text for more details.

Fig. 5 shows that the peak position obtained from the structure of tactoids changes slightly from Na^+ to Ca^{2+} to La^{3+} montmorillonites, corresponding to an increase in the repeat distance from 1.87 to 1.95 nm. One could tentatively ascribe this increase to a larger hydration shell for the more highly charged cation, which leads to an expansion of the water layers to 0.95 nm. Interestingly, here, the number of platelets per tactoid remains close to 20 for all three ions, as a result of using a fractionated dispersion of Na montmorillonite platelets with $D_{eff} \simeq 900$ nm.

A completely different picture emerges in the presence of 100 mM aluminum chloride solution. In Fig. 5, the peak at $q \approx 3.2$ nm^{-1} is still there but a shoulder at $q \approx 2.9$ nm^{-1} appears corresponding to an increase of the water layers of approximately 0.3 nm. Here, it should be noted that the diffuse peaks in the presence of $AlCl_3$ was recorded after a week,

whereas the dispersion of Na montmorillonite that equilibrated at pH 2 has been measured by SAXS after 3 months. In the latter case, a single peak corresponds to a maximum thickness of water layers of about 1.2 nm is observed, indicating a significant change in the repeat distances from 1.95 to 2.2 nm. Thus, the spectra in Fig. 5 can be used to explain the formation of aluminum poly-nuclear complexes passing through the intermediate step *i.e.* from the diffuse peaks to more pronounced and sharp one over the time period. The reasons behind the difference of the observed repeat distances for La and Al montmorillonites have also been investigated by MC simulations. Assuming that nothing else in La montmorillonite dispersion changes, simulations would predict then stronger interactions between the platelets and a distinct peak, in agreement with SAXS curve (see open circles). While in low acidic conditions a gradual dissolution of montmorillonite platelets takes place so that Al^{3+} ions are released and hydrated to different degrees both in size and shape, then eventually replace Na^{+} counterions. Oades[41] and Rich[42] clearly showed that Al^{3+} ions contribute to reducing the overall negative charge density of clay platelets. Simulations then would predict the observed behavior and below we will try to quantify this effect in more details.

Swelling of Montmorillonite in Neutral and Acidic pH

Fig. 6a shows the swelling of Na montmorillonite in pure water at different acidity. As can be seen, the swelling is greatly reduced at low pH. One possible explanation could be that the amount of edge charges increases due to titrating groups, but knowing that silicate nanoplatelets slowly dissolve at low pH (see Table 1) it is more likely that the release of Mg^{2+} and Al^{3+} ions is the main cause of reducing the swelling. In other words, the divalent and trivalent ions replace the Na^{+} ions as counterions so that the ordinary double layer repulsion is converted into a net attraction due to ion-ion correlations.[32] This results in the formation of tactoids, where a limited number of platelets aggregate into a parallel arrangement with a few water layers in between, the so-called intra-lamellar swelling. There is, however, still a significant extra-lamellar swelling among the tactoids and this is in fact responsible for the

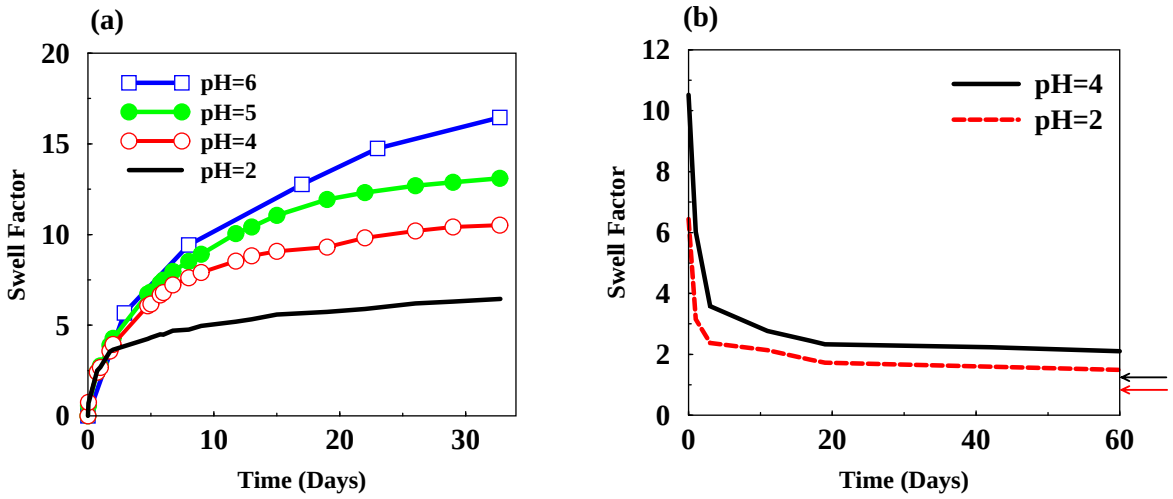

Fig. 6: (a) Dry Na montmorillonite was placed in a dialysis pocket and immersed in deionized water at different pH as indicated in the graph. (b) Deswelling of a Na montmorillonite in salt free solution. After one month in pure water, the pockets were immersed in an aqueous solution containing 4 wt% of polyethylene glycol at pH=2 (dashed line) and at pH=4 (solid line). The arrows indicate the swelling level after six months. The swell factor is the mass ratio of water to clay.

overwhelming part of the water uptake observed. Thus, the micron-sized aggregates seen in Fig. 1. are essentially formed from several tactoids.

The extra-lamellar swelling is easily provoked by a stressing agent and Fig. 6b shows how a 4 wt% polyethylene glycol (PEG) solution can dewater the dispersions. The arrows in Fig. 6b show that after six months montmorillonite dispersions at pH=2 and pH=4 contain 0.83 and 1.24 g water/g clay, respectively. With an approximate clay density of 2.8 g/cm^3, a clay layer thickness of 0.9 nm and a tactoid size of 9 we can estimate the water layer thickness *between* the tactoids to approximately 9 nm at pH 2. At pH 4 we can not estimate the tactoid size accurately from Fig. 3b, however, knowing that the osmotic pressure in Fig. 6b is roughly the same at pH 2 and 4, we can use the data to estimate $\langle N \rangle \approx 4$. This is not an unreasonable number, since at pH 3 we find $\langle N \rangle \approx 6$.

The equation of state for PEG[39] gives $\Pi \approx 5 - 10$ kPa. We can, for instance, take the system at pH 2 and assume that the bulk contains 25 mM of NaCl and 0.1 mM of $AlCl_3$. For this system, simulations predict a pressure less than 1 kPa and in the absence of salt a lower pressure is found in the simulations. Thus, we may conclude that the experimental pressure does not come from an ideal lamellar system, but it is due to the presence of

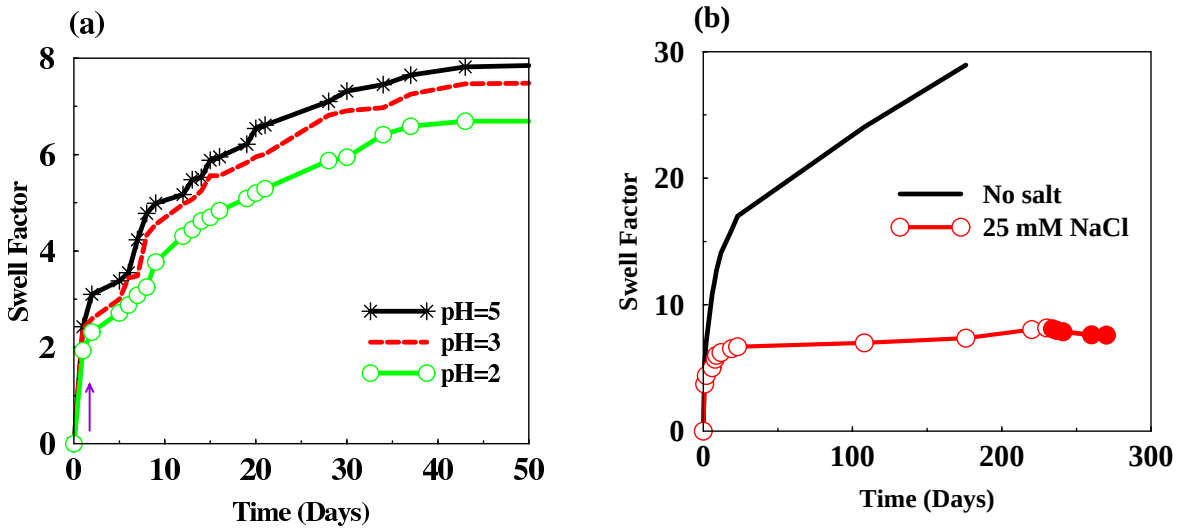

Fig. 7: (a) Dialysis pockets of Na montmorillonite immersed initially in 0.3 M NaCl solutions at different acidity. After one week, (see arrow) the pockets were transferred to 30 mM NaCl solutions to monitor the swelling at different pH as indicated in the graph. (b) Na montmorillonite in deionized water at pH=6 (solid line) and in 25 mM NaCl electrolyte solution at pH=6 (open circles). The latter pocket was immersed in 25 mM NaCl solution at pH=4 after 230 days (filled circles).

small-sized clay platelets. These nanoplatelets do not penetrate the dialysis membrane but remain in the pocket and are responsible for the extra-lamellar swelling of montmorillonite dispersions. This is in agreement with the observation found recently in unfractionated Ca montmorillonite dispersion, where the presence of large proportion of small nanoplatelets increases the extra-lamellar swelling in the system.[40]

Montmorillonite platelets in salt solution react qualitatively in the same way at both neutral and low pH, see Fig. 7. The salt effect is of course larger at neutral pH, since here the clay has taken up more water than at acidic conditions. Fig. 7b shows swelling properties of Na montmorillonite in salt and salt free systems, where the swelling has been followed for almost a year. In salt free solution and pH=6, the swelling is completely unhindered, while with 25 mM NaCl the swelling rate is significantly reduced after a month with a swell factor of 7−8. The limited swelling in 25 mM NaCl could be due to attractive interactions (overlapping) between positive edge charges and the negatively charged faces of the platelets. Lowering pH from 6 to 4 after seven months has virtually no effect on the swelling.

Free Swelling Characterization

Fig. 8 demonstrates the previous findings on a macroscopic scale. In tube (a) Na montmorillonite forms a stable gel incorporating the total aqueous solution.[43,44] This corresponds to the limited swelling seen in Fig. 7b. Reducing clay volume fraction, as done in tube (e), leads to the formation of two phases, *i.e.* one gel phase and on top of that an almost clear aqueous phase. Tube (b) shows both a swollen phase and a precipitate at the bottom indicating the formation of large aggregates due to an exchange of the monovalent sodium counterions with the released divalent, in agreement with SAXS data in Fig. 3 and Table 1. Tube (d) is only a dilution of tube (b). Finally, tube (c) is similar to (e) with a gel phase and a clear top phase. This is consistent with the swelling data, where a clay at pH=4 and 6 in 25 mM NaCl shows the same limited swelling level (see open and filled circles in Fig. 7b).

Parameter	(a)	(b)	(c)	(d)	(e)
pH	6	4	4	4	6
c_s (mM)	25	0	25	0	25
ϕ_c (%)	1	1	0.3	0.3	0.3

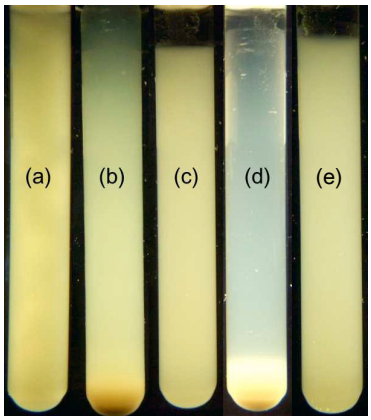

Fig. 8: Snapshots of Na montmorillonite dispersions with varying clay volume fraction, ϕ_c. The samples have been equilibrated in the tubes for four months. The experimental conditions for the five samples (a−e) are shown in the table above.

Simulation Results

The dramatic change of clay properties in terms of swelling and hydraulic conductivity is strongly correlated to the appearance of tactoids. The aggregation is driven by a net attractive interaction between the negatively charged platelets. A net attractive interaction between equally charged colloids or particles is typically found in systems with di- or multivalent counterions. When it comes to simulate clay platelets, there is a lacking in the precise value of the surface charge density and how it changes with different pH. According to ICP-AES analysis, the concentrations of mono-, di- and trivalent cations in the bulk solution at pH=2 are 48, 126 and 180 μM, respectively. We will use this as a reference solution in simulation set *A*. Here we have lumped Ca^{2+}, Mg^{2+} and Fe^{2+} into the divalent group. In a second set of simulations, *B*, we assumed that all aluminum ions effectively appear as divalent species due to complexation with OH^-. The corresponding bulk concentrations of mono- and divalent cations will then be 48 and 306 μM, respectively.

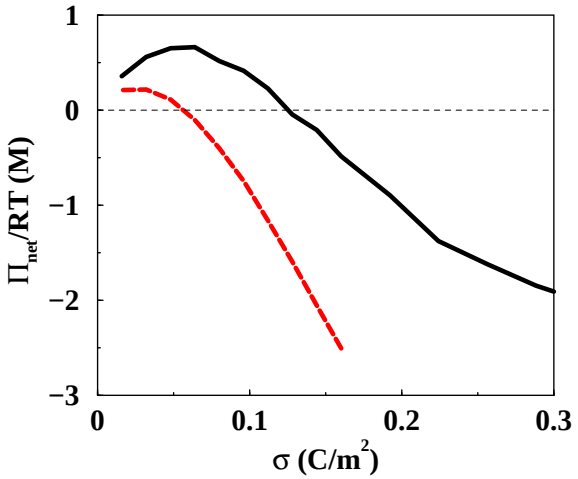

Fig. 9: The net osmotic pressure as a function of surface charge density at a platelet-platelet separation of 1 nm. The bulk solution contains 180 μM trivalent cations, 126 μM divalent cations and 30 mM monovalent cations (black solid line). The red dashed line is for a bulk with 306 μM divalent cations and 30 mM monovalent cations. The bulk anion is in both cases monovalent.

Fig. 9 shows how the net osmotic pressure varies as a function of surface charge density and counterion valency in the bulk. One can see that the transition from attractive to repulsive pressure takes place approximately at the estimated clay surface charge density or

slightly below depending on counterion valency. With dominating trivalent counterions in the bulk, the transition is found at $\sigma \approx 0.06$ C/m^2, while with mainly divalent counterions as in simulation set B the turnover from repulsion to attraction takes place at $\sigma \approx 0.12$ C/m^2. An interesting observation is that the pressure curves in Fig. 9 display maxima at low surface charge density. That is, there is an optimal swelling capacity at this charge density. Both systems in Fig. 9 contain a significant amount of monovalent cations, still the pressures are strongly attractive for most surface charge densities. This reflects that the competition between monovalent and multivalent counterions wins by the latter. In simulation set A with trivalent Al^{3+} competing with monovalent Na^+ ions, the latter bulk concentration needs to be approximately 1000 higher than the former in order to obtain equal concentrations of the two counterions close to the clay surface. In simulation set B the surface charge density is higher, but the competition is on the other hand between di- and monovalent cations and the final result is qualitatively the same. That is, the bulk concentration of monovalent cations needs to be much higher than the di- or trivalent cation concentration.

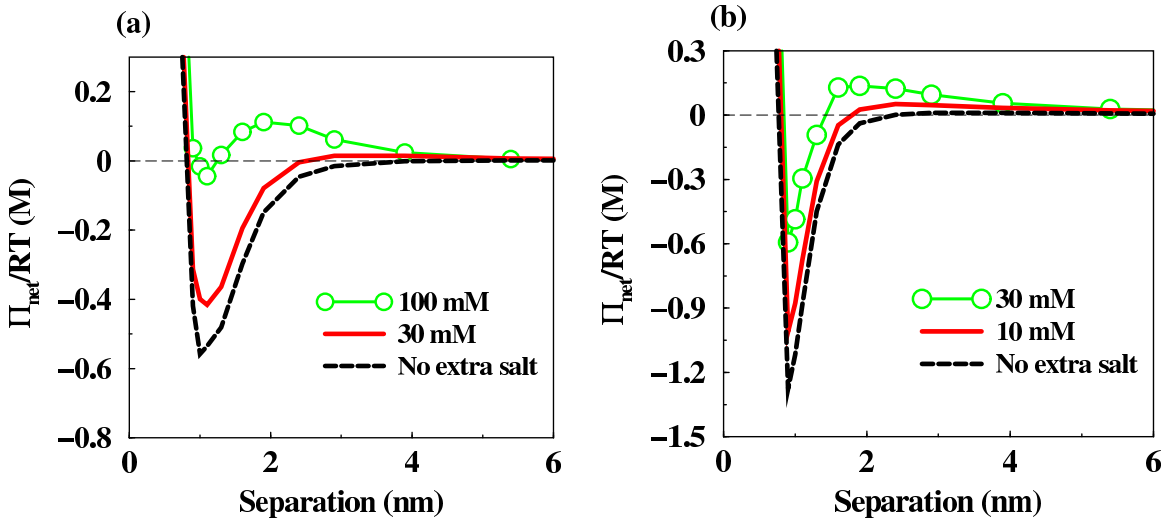

Fig. 10: The net osmotic pressure as a function of separation for the two simulation sets A and B. The concentration of 1:1 salt in the bulk is indicated in the graph. (a) The surface charge density is 0.08 C/m^2 and the bulk contains 180 μM trivalent cations and 126 μM divalent cations in addition to the 1:1 salt. (b) The surface charge density is 0.16 C/m^2 and the bulk contains 306 μM divalent cations in addition to the 1:1 salt. The bulk anion is in all cases monovalent.

Fig. 10 shows the net osmotic pressure as a function of separation. Both simulation sets, A with dominant trivalent counterions and B with dominant divalent counterions, show

the same qualitative behavior with a distinct minimum at approximately 1 nm separation in agreement with experiments. At larger separation the classical entropic double layer repulsion takes over. By adding monovalent counterions to the bulk, we create a competition situation, where the tri- and divalent counterions gradually become exchanged with monovalent ones. At the same time the attraction slowly turns into repulsion for sufficiently high concentration of monovalent cations in the bulk. The influence of this change is also seen above in Fig. 3 and 4, where the tactoid size decreases due to the addition of NaCl to the bulk solution. In general, higher valency leads to stronger correlation and thinner water

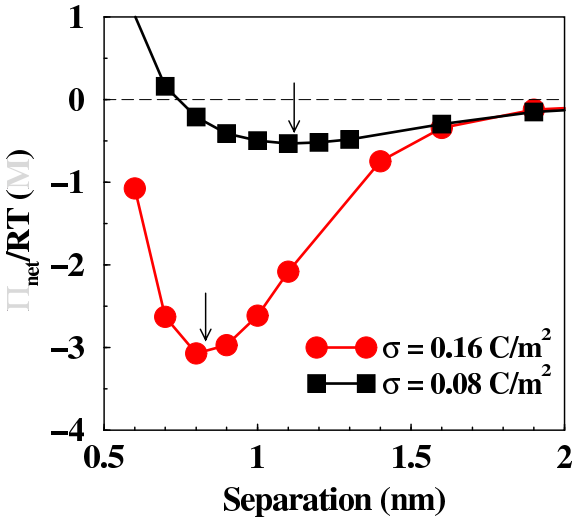

Fig. 11: The net osmotic pressure as a function of separation for a system in equilibrium with a bulk dominated by trivalent counterioins. Here, no extra salt is added. The surface charge density is varied as indicated in the graph and the arrows indicate force minima.

layers, while a reduced surface charge density decreases the ion-ion correlations resulting in an increased water layer thickness. Fig. 11 shows a detailed comparison between two simulations with the same bulk, but with different surface charge density. This is supposed to mimic the difference between La^{3+} montmorillonite on one hand and Na^{+} montmorillonite at pH 2 on the other hand. In the latter case, Al^{3+} ions are released, hydrated and polymerized, hence this reaction is accompanied by a decrease in surface charge density and the cation exchange capacity (CEC).[41,42] As seen in Fig. 11, the minimum of the osmotic pressure curve is shifted outwards by approximately 0.3 nm in agreement with the scattering results in Fig. 5.

Conclusions

Montmorillonite platelets dissolve slowly at low pH and in this process trivalent Al^{3+} ions are released, polymerized and can replace the original counterion be it Na^+ or Ca^{2+}. A consequence is that, silicate platelets aggregate into tactoids where the average number of platelets per tactoid is rather limited $\langle N \rangle \simeq 6 - 9$. The size of montmorillonite platelets is reduced slightly due to the dissolution process. The swelling capacity is decreased, but there is still a significant extra-lamellar swelling among the tactoids. The repulsion forces acting in the extra-lamellar swelling can be explained by the presence of small or very small nanoplatelets, as such platelets do not form tactoids.[40] When Al^{3+} replaces Na^+ as counterion under acidic condition, there is a change in the scattering peak position corresponding to an increase of the intra-lamellar swelling, which can be explained by a reduction of surface charge density. The strong ionic competition between mono-, di- and trivalent counterions as well as the net attraction is a consequence of ion-ion correlations, which in turn driving the formation of tactoid, as predicted by Monte Carlo simulations.

Acknowledgment

This study was financed by the Swedish Research Council through the Linnaeus grant Organizing Molecular Matter and partly funded by the Swedish Nuclear Fuel and Waste Management Company (SKB). M. Segad gratefully acknowledges the Royal Physiographic Society of Lund (KFS) for a number of grants including the Birgit and Hellmuth Hertz'. M. Segad also wants to express his appreciation to Z. Kaleh for joining the beamtime at MAX IV Laboratory in Lund, Sweden. Kelly Marino and Leslie Krauss are thanked for assistance with the hyperspectral imaging. Bo Jönsson wants to express his appreciation for the interesting discussions with the personnel at ClayTech, Lund. This work is dedicated to Torbjörn Åkesson who passed away.

References

(1) H. van Olphen, *An Introduction to Clay Colloid Chemistry*, 2nd Ed.; John Wiley and Sons Inc.: New York, 1977.

(2) H. Freundlich, O. Schmidt and G. Lindau, *Kolloidchem-Beihefte*, 1932, **36**, 43-81.

(3) U. Hofmann and A. Hausdorf, *Kolloid-Z.*, 1945, **110**, 1-17.

(4) I. Langmuir, *J. Chem. Phys.*, 1938, **6**, 873-896.

(5) H. van Olphen, *J. Coll. Sci.*, 1962, **17**, 660-667.

(6) G. Keled, J. Hári and B. Pukánszky, *Nanoscale*, 2012, **4**, 1919-1938.

(7) K. Oh, Y. P. Seo, S. M. Hong, A. Takahara, K. H. Lee and Y. Seo, *Phys. Chem. Chem. Phys.*, 2013, **15**, 11061-11069.

(8) C. Breen and A. Moronta, *J. Phys. Chem.*, 2000, **4**, 2702-2708.

(9) C. Breen and A. Moronta, *J. Phys. Chem. B*, 1999, **103**, 5675-5680.

(10) J. Mulder and J. J. M. van Grinsven, *Soil Sci. Soc. Am. J.*, 1987, **51**, 1640-1646.

(11) J. N. Mukherjee, *Nature*, 1922, **110**, 732-732.

(12) J. N. Mukherjee and B. C. Roy, *J. Chem. Soc. Trans.*, 1924, **125**, 476-488.

(13) H. B. Weiser and G. R. Gray *Phys. Chem.*, 1932, **36**, 2217-2193.

(14) H. Jenny and R. F. Reitemeier, *J. Phys. Chem.*, 1935, **39**, 593-604.

(15) D. Russo and E. Bresler, *Soil Sci. Soc. Am. J.*, 1977, **41**, 706-710.

(16) H. Komine, *Appl. Clay Sci.*, 2004, **26**, 13-19.

(17) D. Guyonnet, E. Gaucher, H. Gaboriau, C.-H. Pons, C. Clinard, V. Norotte and G. J. Didier, *J. Geotech. Geoenv. Eng.*, 2005, **131**, 740-749.

(18) K. Norrish, *Disc. Faraday Soc.*, 1954, **18**, 120-134.

(19) I. Shainberg, E. Bresler and Y. Klausner, *Soil Sci.*, 1971, **5**, 214-219.

(20) I. C. Callaghan and R. H. Ottewill, *Faraday Disc.*, 1974, **57**, 110-118.

(21) E. Paineau, I. Bihannic, C. Baravian, A.-M. Philippe, P. Davidson, P. Levitz, S. S. Funari, C. Rochas and L. J. Michot, *Langmuir*, **2011**, **27**, 5562-5573.

(22) M. Segad, Bo Jönsson, T. Åkesson and B. Cabane, *Langmuir*, 2010, **26**, 5782-5790.

(23) M. Segad, S. Hanski, U. Olsson, J. Ruokolainen, T. Åkesson, Bo Jönsson, *J. Phys. Chem. C*, 2012, **116**, 7596-7601.

(24) M. Segad, Bo Jönsson and B. Cabane, *J. Phys. Chem. C*, 2012, **116**, 25425-25433.

(25) M. Knaapila, C. Svensson, J. Barauskas, M. Zackrisson, S. S. Nielsen, K. N. Toft, B. J. Vestergaard, L. Arleth, U. Olsson, J. S. Pedersen and Y. A. Cerenius, *J. Synchrotron Radiat.*, **2009**, **16**, 498-504.

(26) A. P. Hammersley, S. O. Svensson, A. Thompson, H. Graafsma, E. Kvick and J. P. Moy, *Rev. Sci. Instr.*, 1995, **66**, 2729-2733.

(27) A. L. Patterson, *Phys. Rev.*, 1939, **56**, 978-928.

(28) M. Segad, *J. Appl. Cryst.*, 2013, **46**, 1316-1322.

(29) R. Kjellander, S. Marčelja, and J. P. Quirk, *J. Coll. Interf. Sci.*, 1988, **126**, 194-211.

(30) A. Kahn, *J. Coll. Sci.*, 1958, **13**, 51-60.

(31) J. P. Valleau, R. Ivkov and G. M. Torrie, *J. Chem. Phys.*, 1991, **95**, 520-532.

(32) L. Guldbrand, Bo Jönsson, H. Wennerström and P. Linse, *J. Chem. Phys.*, 1984, **80**, 2221-2228.

(33) M. P. Allen and D. J. Tildesley, *Computer Simulation of Liquids*, Oxford University Press: Oxford, 1989.

(34) D. Frenkel and B. Smit, *Understanding Molecular Simulation*, Academic Press: San Diego, 1996.

(35) B. Widom, *J. Chem. Phys.*, 1963, **39**, 2808-2812.

(36) C. Tournassat, J.-M. Greneche, D. Tisserand and L. Charlet, *J. Coll. Interf. Sci.*, 2004, **273**, 224-233.

(37) L. Charlet and C. Tournassat, *Aquatic Geochemistry*, 2005, **11**, 115-137.

(38) M. L. Rozalen, F. L. Huertas, P. V. Brady, J. Cama, S. García-Palma and J. Linares, *Geochimica et Cosmochimica Acta*, 2008, **72**, 4224-4253.

(39) A. Bouchoux, P. E. Cayemitte, J. Jardin, G. Gezan-Guiziou and B. Cabane, *Biophys. J.*, 2009, **96**, 693-706.

(40) M. Segad, B. Cabane and B. Jönsson, *Nanoscale*, DOI: 10.1039/C5NR04615G.

(41) J. M. Oades, *Clay and Clay Minerals*, 1984, **32**, 49-57.

(42) C. I. Rich, *Soil Sci. Soc. Am. J.*, 1960, **24**, 26-32.

(43) M. Segad Meehdi, *Synchrotron X-ray Scattering and Monte Carlo Simulations of Structure and Forces in Silicate Nano- platelet Dispersions*, Doctoral dissertation, Lund University, Lund, Sweden, 2014.

(44) R. Eriksson and T. Schatz *Applied Clay Science*, 2015, **108**, 12-18.

TOC

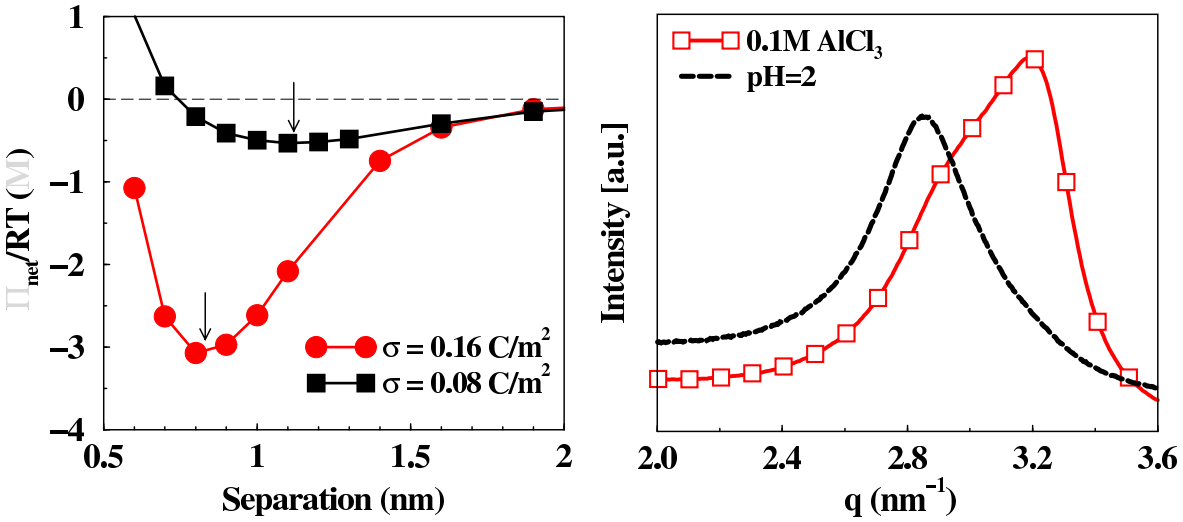

Montmorillonite platelets dissolve slowly at low pH and among other species trivalent Al^{3+} ions are released, hydrated and polymerized. The dissolution process dramatically changes the microstructure of Na montmorillonite, which instead of having fully exfoliated platelets, turns into a structure of aggregated platelets, so-called tactoids. This reaction is accompanied by a decrease in the surface charge density leading to expand the thickness of water layers into the tactoids.